IEEE Photonics Journal
An IEEE Photonics Society Publication

Open Access

Experimental Investigation of Gain Offset Behavior of Feedforward-Controlled WDM AGC EDFA Under Various Dynamic Wavelength Allocations

Volume 8, Number 1, February 2016

Kiyo Ishii, Member, IEEE
Junya Kurumida, Member, IEEE
Shu Namiki, Senior Member, IEEE

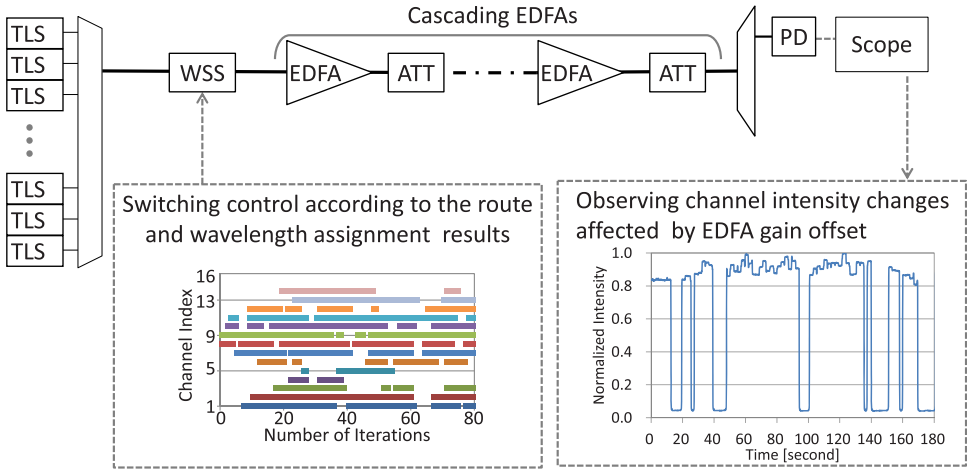

DOI: 10.1109/JPHOT.2016.2514487
1943-0655 © 2016 IEEE

IEEE photonics SOCIETY

IEEE

Experimental Investigation of Gain Offset Behavior of Feedforward-Controlled WDM AGC EDFA Under Various Dynamic Wavelength Allocations

Kiyo Ishii, *Member, IEEE*, Junya Kurumida, *Member, IEEE*, and Shu Namiki, *Senior Member, IEEE*

National Institute of Advanced Industrial and Science Technology, Tsukuba 305-8568, Japan

DOI: 10.1109/JPHOT.2016.2514487

Manuscript received December 8, 2015; revised December 30, 2015; accepted December 31, 2015. Date of publication January 4, 2016; date of current version February 9, 2016. This work was supported in part by the Project for Developing, Innovation Systems of the Ministry of Education Culture, Sports, Science, and Technology (MEXT), Japan. Corresponding author: K. Ishii (e-mail: kiyo-ishii@aist.go.jp).

Abstract: Realizing dynamics in the optical layer is becoming more important for efficient optical communication networks such as protection switching in the optical domain or reconfiguring the optical layer to meet traffic fluctuations. This paper experimentally investigates gain offset changes under dynamic optical switching using feedforward-controlled wavelength-division-multiplexing (WDM) automatic gain control erbium-doped fiber amplifiers (EDFAs). Realistic optical switching scenarios are emulated by resolving dynamic routing and wavelength assignment problems. The experimental results demonstrate that channel intensity changes with optical switching and that the intensity changes accumulate as the number of cascaded EDFAs increases. Considering a gain model in wavelength assignment can successfully reduce the channel intensity changes by up to 0.7 dB after five cascaded EDFAs. Effects of gain spectral hole burning on the intensity changes are also discussed.

Index Terms: Optical communications, fiber optics systems.

1. Introduction

Agile and reconfigurable wavelength-division-multiplexing (WDM) optical communication network systems are becoming more important for achieving low cost and energy efficiency, such as protection switching in optical domain or reconfiguring the optical layer to meet traffic fluctuations [1]–[3]. In these systems, optical or wavelength channel paths are dynamically established or deleted according to traffic demands. Such dynamic optical-switching operations change the allocations of wavelengths, as well as the total optical power in each optical link. Consequently, the input conditions of optical amplifiers on the link are dynamically changed; and thus suppressing gain changes in optical amplifiers due to the input changes is one of the most essential technologies enabling such dynamic and agile optical path switching network systems. To maintain a constant gain for arbitrary input wavelength conditions, the use of automatic gain control (AGC) erbium-doped fiber amplifiers (EDFAs) is needed.

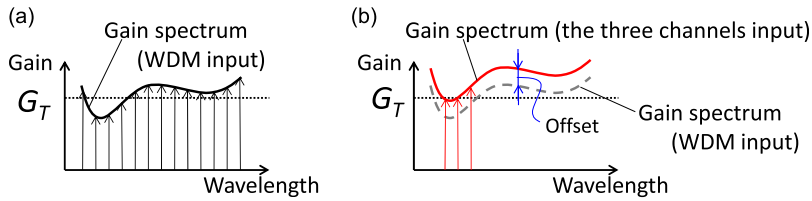

Fig. 1. Principle of gain offset in AGC WDM EDFA. (a) WDM input. (b) Three channels input with a corresponding gain spectrum.

However, even with a perfect implementation of fast electronic gain control, WDM AGC EDFAs still suffer from two kinds of gain changes under dynamic optical switching. The first gain change is an optical surge resulting from the intrinsic transient response of EDFAs such as overshoot and undershoot [4]–[6]. To suppress such gain transients, various promising technologies have been proposed and experimentally demonstrated [7]–[14]. We have also shown that a fast electrical feed-forward control can significantly reduce fast gain transients without oscillatory responses under a condition of cascading EDFAs. Furthermore, we have demonstrated that a fast variable optical attenuator (VOA) can help suppress accumulated transients [15], [16].

The second gain change is a gain offset that originates from gain spectrum ripples and a dependence of the gain flatness on input wavelength allocations caused by the gain spectral hole burning (GSHB) effect due to homogeneous and inhomogeneous gain saturation [6], [17], [18], [22]–[25]. Although gain offset has been commonly recognized as a significant phenomenon, detailed experimental investigations on its behavior under a condition of dynamic optical switching have not been reported to date. So far, gain offsets have been addressed on a case-by-case basis because optical paths have been operated statically rather than dynamically. Comprehensive investigations of gain offsets during dynamic optical switching and methods of suppression must be developed to realize dynamic optical switching and efficient optical communication systems.

In this paper, we experimentally investigate the gain offsets under a condition of dynamic optical switching. To emulate practical wavelength-switching scenarios, we resolve routing and wavelength assignment (RWA) problems with randomly generated dynamic wavelength demands, and we examine five different policies of wavelength assignment. Gain offset behaviors are experimentally investigated with the obtained wavelength-switching scenarios. Experimental results show that the assignment policy considering a gain model can reduce the effect of the gain offsets by 5–15% (0.3–0.7 dB) after five cascaded EDFAs. This paper extends our previous work in [19] by providing additional experimental results and discussions about the effects of GSHB and presenting comprehensive formulations of the RWA. The rest of the paper is organized as follows. Section 2 briefly explains the principle of the gain offset in AGC EDFAs. Section 3 describes the characteristics of a feedforward-controlled AGC EDFA used in our experiments and presents a simple model of the gain behavior. Though the gain model does not take into account the GSHB effect, the effect is experimentally evaluated in Section 3. Section 4 describes the dynamic RWA algorithm and the assignment results as the obtained switching scenarios. Section 5 demonstrates the experiments of evaluating the EDFA offsets with dynamic optical switching. Following the conclusion in Section 6, detailed formulations used in the dynamic RWA are provided in the Appendix.

2. Principle of the Gain Offset

AGC EDFAs dynamically adjust the pump power to maintain a constant gain by monitoring total input and output powers. For a single-channel input, an AGC EDFA can achieve a constant target gain G_T for any wavelength with a feedback control. However, because of residual gain ripples, the gain offset can occur in WDM input conditions, as shown in Fig. 1. In Fig. 1(a), all of the WDM channels are input to the EDFA and the target gain G_T is achieved on average. In Fig. 1(b), only three channels are input and the target gain G_T is also achieved on average

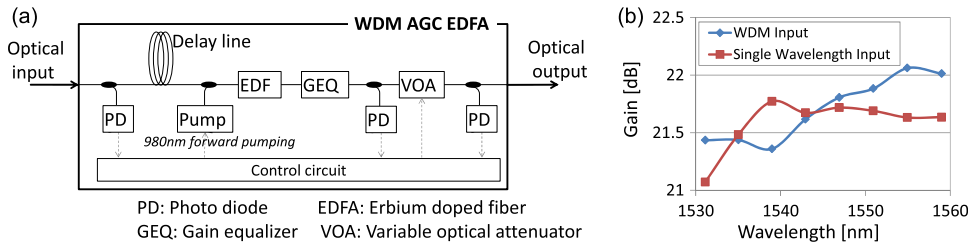

Fig. 2. Features of the WDM AGC EDFA with fast electrical feed-forward control used in this paper. (a) Configuration of the EDFA [7], [27] and (b) gain curves of the EDFA for WDM input and single-wavelength input.

since the AGC adjusts the pump power with a feedback control. However, according to the gain spectrum for WDM input, the three channels experience smaller gain than other channels. As a result, the three channels experience larger gain in the condition of the three channels input [see Fig. 1(b)] than in that of WDM input [see Fig. 1(a)]. This offset originates from the residual gain ripples due to imperfections in the gain equalizing (GEQ) filter.

A simple mathematical expression of this gain behavior is given as

$$\hat{g}(\lambda_i) = g(\lambda_i) + \frac{\sum_{j=1}^{n}\{G_T - g(\lambda_j)\}}{n} \tag{1}$$

where $\hat{g}(\lambda_i)$ represents the gain experienced by the wavelength $\lambda_i \in \{\lambda_1, \ldots, \lambda_n\}$ when a wavelength set $\{\lambda_1, \ldots, \lambda_n\}$ is input to the EDFA, and $g(\lambda_i)$ represents the gain experienced by the wavelength λ_i when all of the WDM channels are input to the EDFA. In addition to imperfections in the GEQ filter, the GSHB causes further gain errors because it changes the gain curve according to the input wavelength conditions. In (1), for simplicity, the GSHB effect is not considered.

3. Gain Offset in a WDM AGC EDFA With a Fast Electrical Feedforward Control

3.1. Characteristics of the EDFA Used in this Paper

Fig. 2 shows the features of the WDM AGC EDFA used in this paper. The configuration is shown in Fig. 2(a). The EDFA employs single-stage 980-nm forward pumping. A fast electrical feedforward control and a relatively slow feedback control are implemented to suppress the instantaneous gain transients and to avoid oscillatory responses at the same time [15]. The gain, noise figure, input optical power range, operation wavelength range, and gain flatness are specified as $\geq$ 20 dB, $\leq$ 7 dB, –23 to –4 dBm, 1530 to 1560 nm, and $\leq \pm 1$ dB, respectively. The EDFA has a GEQ filter to flatten the gain spectrum. The gain characteristics are illustrated in Fig. 2(b). The gain curve for WDM input indicates that the residual gain ripple of this EDFA is approximately 0.6 dB. In the gain curve for single-channel input, the gain for 1530–1540 nm wavelengths is decreased by approximately 0.7 dB. The EDFA is mainly controlled with feedforward and the pump power is determined based on the input optical power rather than the output optical power. Hence the pump power does not increase enough to compensate for the GSHB effect for the input wavelength range of 1530 to 1540 nm. The fast variable optical attenuator (VOA) at the output side enhances the suppression of the instantaneous transients caused by fast optical switching [15], [20]. The fast VOA does not affect the gain-offset characteristics. The noise figure of $\leq$ 7 dB is in a common range for commercially available WDM EDFAs and the degradation of the noise figure or OSNR due to the optical couplers for power monitoring, the fiber delay line, and the VOA is marginal. The delay caused by the fiber delay line for adjusting the timing is negligible for the use of long-haul transmission.

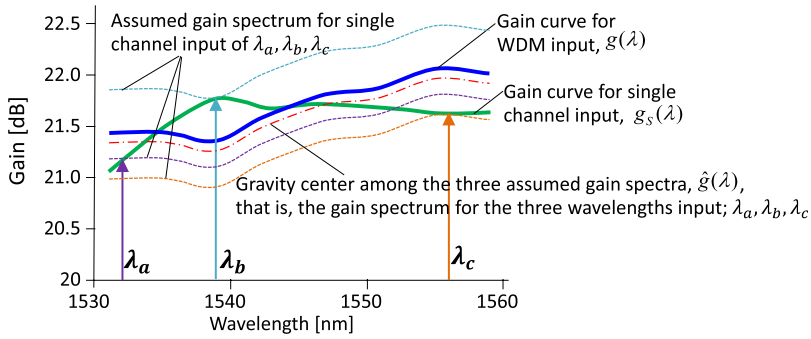

Fig. 3. Simple gain model expressed in (2).

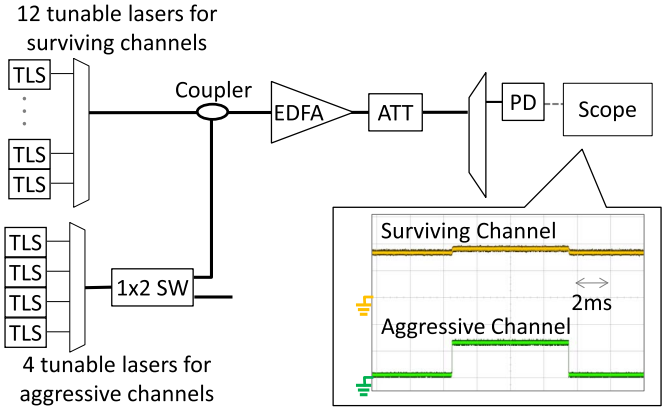

Fig. 4. Experimental setup for evaluation of the gain model. The inset shows examples of measured waveforms.

3.2. Gain Modeling

As shown in Fig. 2(b), the feedforward-controlled AGC EDFA used here does not achieve a constant target gain for single wavelength input, unlike the feedback-controlled AGC EDFAs that were explained in Section 2. According to this difference, we modify (1) to express our EDFA as

$$\hat{g}(\lambda_i) = g(\lambda_i) + \frac{\sum_{j=1}^{n} \{g_S(\lambda_j) - g(\lambda_j)\}}{n} \tag{2}$$

where $g_S(\lambda_j)$ represents the gain experienced by the wavelength λ_j when only λ_j is input to the EDFA. We use $g_S(\lambda_j)$ instead of G_T, which represents the gain curve for single-wavelength input in feedback-controlled AGC EDFAs as well as the target gain. In (2), we assume that the gain spectrum is not modified by the input wavelength change, as shown in Fig. 3. The gain spectrum is indeed modified according to the input wavelength conditions because of wavelength-dependent saturation or GSHB. Despite this, we will show that a wavelength-assignment policy based on this simple model without considering the GSHB effect can reduce the effects of the gain offsets under a condition of dynamic wavelength switching. This model can be easily modified for other EDFAs.

3.3. Experimental Evaluation of the Gain Model

Fig. 4 shows the experimental setup for evaluating the gain model in (2). Twelve wavelengths are continuously input to the EDFA; we call these surviving channels. Four wavelengths are intermittingly input to the EDFA with a 1 $\times$ 2 optical switch to emulate an operation of dynamic optical switching; we call these aggressive channels. The channel power was set to –23 dBm/

TABLE 1

Channel Allocations for Gain Model Evaluation

	(i) Short	(ii) Shorter Center	(iii) Longer Center	(iv) Long
Aggressive Channels	1530.334	1537.397	1545.322	1553.329
	1531.898	1538.976	1546.917	1554.94
	1533.465	1540.557	1548.515	1556.555
	1535.036	1542.142	1550.116	1558.173
Surviving Channels [nm]	1531.116	1531.116	1531.116	1531.116
	1532.681	1533.465	1533.465	1533.465
	1535.822	1535.822	1535.822	1535.822
	1538.186	1538.186	1538.186	1538.186
	1540.557	1539.766	1540.557	1540.557
	1542.936	1542.936	1542.936	1542.936
	1545.322	1545.322	1544.526	1545.322
	1547.715	1547.715	1547.715	1547.715
	1550.116	1550.116	1550.918	1550.116
	1552.524	1552.524	1552.524	1552.524
	1555.747	1555.747	1555.747	1555.747
	1558.983	1558.983	1558.983	1558.983

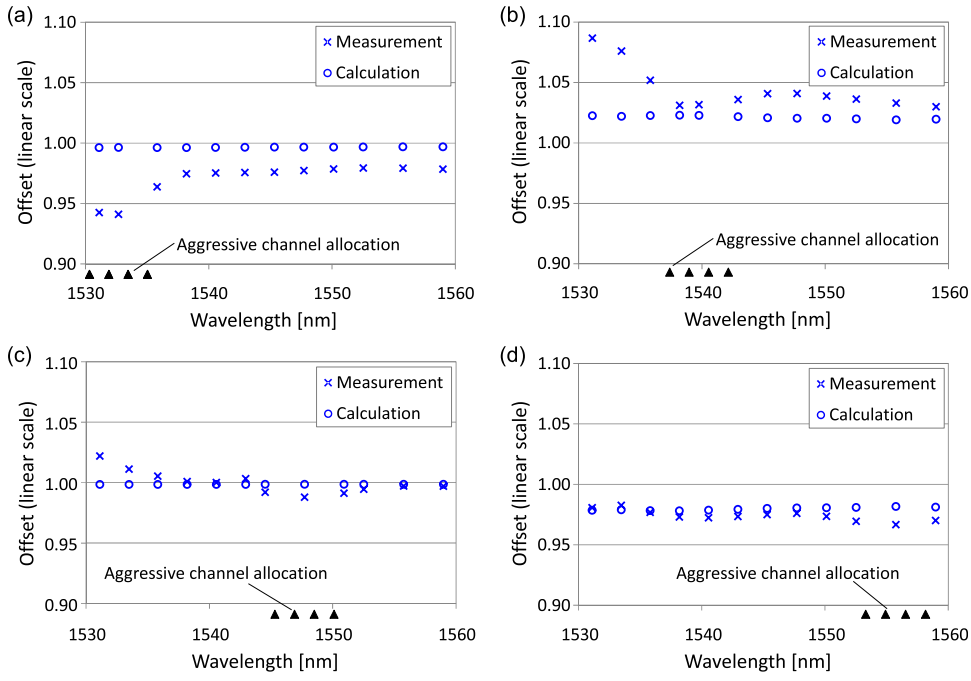

Fig. 5. Experimental results of gain model evaluation for the four wavelength allocations. (a) Short, (b) shorter center, (c) longer center, and (d) long. Triangle marks under the horizontal axis show the aggressive channel allocations.

ch; the total output power of EDFA is about +10 dBm when all aggressive channels are ON and about +9dBm when all aggressive channels are OFF. Examples of measured waveforms shown in the inset of Fig. 4 illustrate that the surviving channel suffers a gain change during the time the aggressive channel is on. We measured the surviving channel gain changes for four wavelength allocation patterns: (i) short, (ii) shorter center, (iii) longer center, and (iv) long, as shown in Table 1.

Fig. 5 shows the measurement results (cross marks) and the corresponding calculated results (circle marks) based on the gain model in (2). The vertical axis, the offset of a wavelength λ, is

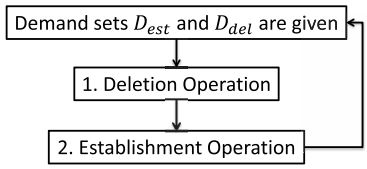

Fig. 6. Flowchart of our RWA for dynamic demands.

given by $P_{\text{Aon}}(\lambda)/P_{\text{Aoff}}(\lambda)$, where $P_{\text{Aon}}(\lambda)$ and $P_{\text{Aoff}}(\lambda)$ represent the EDFA output power or gain of wavelength λ during the time the aggressive channels are on and off, respectively. In Fig. 5, the calculated results are in accordance with the measured results for wavelength channels longer than 1540 nm. It is well known that the gain curve of an EDFA is drastically modified near 1530 nm due to the GSHB effect [18]. In particular, for the wavelength allocation patterns of (iii) longer center and (iv) long, the calculated results agree with the measured results for all 12 surviving channels including the channels shorter than 1540 nm. By contrast, for the wavelength allocation patterns of (i) short and (ii) shorter center, which typically suffer from the large GSHB effect, the gain changes for the surviving channels shorter than 1540 nm were much larger when measured than when calculated. This discrepancy is considered to derive from the gain spectrum changes because of the GSHB effect, which is not taken into account in the gain model of (2). While we have evaluated various other wavelength allocations, numbers of wavelengths, and channel powers, similar trends as shown in Fig. 5 were observed. In particular, experimental results using single surviving channel and multiple aggressive channels, which is one of the worst-case scenarios, were shown in [26].

4. Dynamic Routing and Wavelength Assignment

To generate practical wavelength-switching scenarios, we resolve RWA problems with randomly generated dynamic wavelength demands. Fig. 6 shows a flowchart of the assignment. First, after the establishment demand set D_{est} and deletion demand set D_{del} arrive, the wavelength resources used by the deletion demands are released (deletion operation). Second, wavelength resources are assigned to the establishment demands (establishment operation). Then the next establishment/deletion demand sets arrive, and the deletion and establishment operations are repeated.

In the establishment operation, we resolve optimum resource assignment problems formulated based on link integer linear programming (ILP) [21]. The object function is set to minimize the wavelength resources used to accommodate the given establishment demands. The following five wavelength assignment policies are considered as long as the necessary wavelength resources are not increased.

1. Long: Assign as long wavelengths in the range of operation wavelengths as possible.
2. Short: Assign as short wavelengths in the range of operation wavelengths as possible.
3. Center: Assign as center wavelengths in the range of operation wavelengths as possible.
4. Random: Assign wavelengths randomly.
5. MinDiff: Assign wavelengths as small difference between $g_S(\lambda)$ and $g(\lambda)$ as possible.

The MinDiff policy considers the EDFA gain characteristics to suppress the effect of the gain offsets, while the calculation complexity is the same as the others because of the simple gain model. The detailed formulations are provided in the Appendix.

We employed a 3 $\times$ 3 regular mesh network topology where each link has one duplex fiber. The number of wavelengths per fiber was set to 16. The wavelength allocation was set to be equally spaced on the ITU-T grid from 1533.465 nm to 1557.363 nm. Wavelength conversions were not considered. We generated two traffic patterns: a light traffic pattern and a heavy traffic pattern, as shown in Figs. 7 and 8. The horizontal axis represents the number of iterations where one iteration means a set of operations consisting of an arrival of demand sets, a deletion operation, and an establishment operation as shown in Fig. 6. A demand set D_{est} is generated

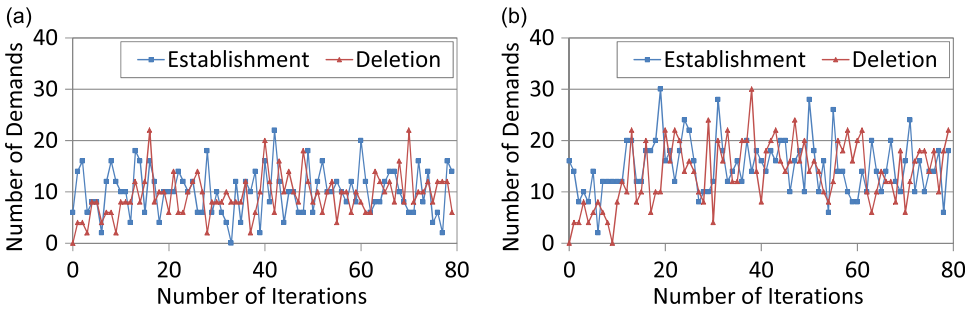

Fig. 7. Number of establishment and deletion demands in the entire network during each iteration. (a) Light traffic and (b) heavy traffic.

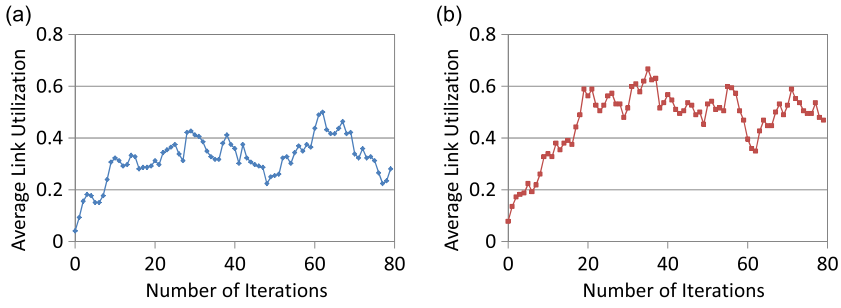

Fig. 8. Average link utilization of (a) light traffic pattern and (b) heavy traffic pattern.

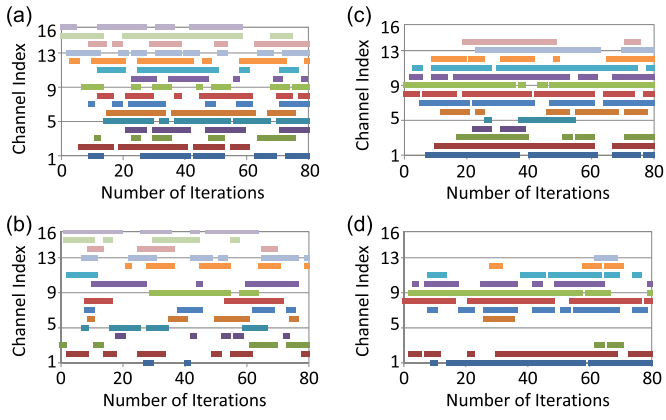

Fig. 9. Example results of wavelength establishment and deletion sequences on a link. (a) and (b) correspond to the Random policy with the heavy and light traffic pattern, respectively. (c) and (d) correspond to the MinDiff policy with the heavy and light traffic pattern, respectively.

for each iteration. Traffic demands for each iteration (that is, elements of D_{est}) were set to be uniformly distributed among node pairs and generated between each node pair following a Poisson distribution. The connection holding time was set to follow a negative exponential distribution.

We used IBM ILOG CPLEX Optimization Studio 12.3 to solve the ILP. Fig. 9 shows the examples of the obtained wavelength path establishment/deletion sequences on a link for the two traffic patterns with the Random policy and the MinDiff policy. In the assignments, blocking (call loss) did not occur since the wavelength resources are enough to accommodate all of the demands. Using these results, we experimentally examine the wavelength dependence of the effects of the EDFA gain offsets, as described in the next section.

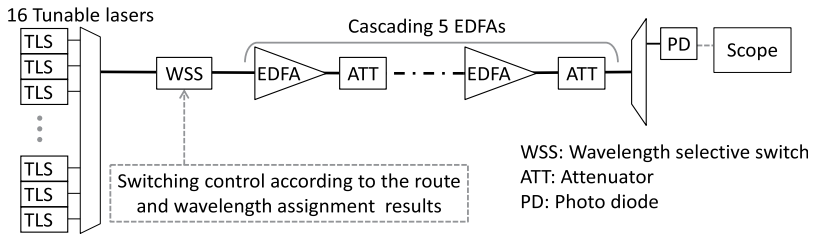

Fig. 10. Experimental setup for evaluating EDFA offset changes caused by dynamic wavelength switching.

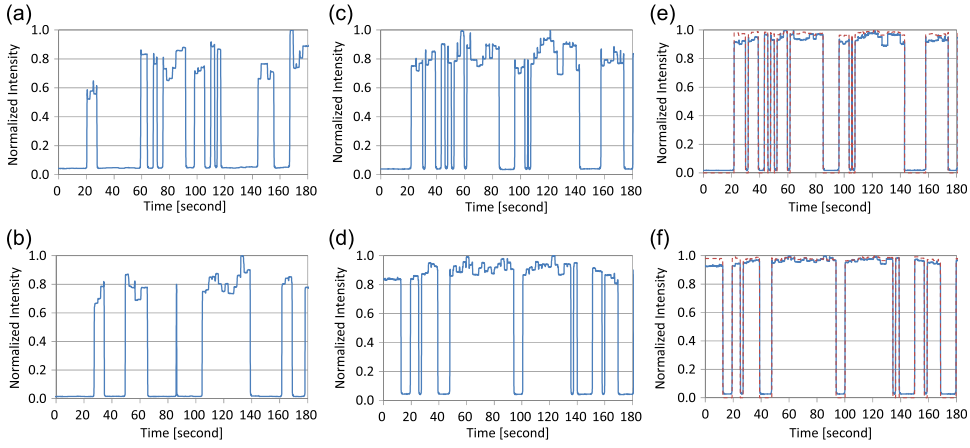

Fig. 11. Examples of measured waveforms with the heavy traffic pattern. (a) and (b) correspond to the Random policy after five EDFAs with Ch. 1 (1533.465 nm) and Ch. 8 (1544.526 nm), respectively. (c) and (d) correspond to the MinDiff policy after five EDFAs with Ch. 1 and Ch. 8, respectively. (e) and (f) correspond to the MinDiff policy after one EDFA with Ch. 1 and Ch. 8, respectively. The dashed line represents the calculated waveform based on the gain model in (2).

5. Experimental Evaluation of the Gain Offset With Practical Wavelength Selective Switching Scenarios

5.1. Experiments

The experimental setup to investigate the EDFA gain offsets under dynamic optical switching is shown in Fig. 10. We used five WDM AGC EDFAs to examine a cascaded condition. The input level of each wavelength channel to the EDFAs was set to –21 dBm/ch. The optical attenuators (ATTs) between the EDFAs emulated either spans or node losses. We used 16 tunable lasers. The wavelengths were set from 1533.465 nm to 1557.363 nm, equally spaced on the ITU-T grid, the same as the wavelength allocation used in the RWA in Section 4. A wavelength selective switch (WSS) was used for switching wavelengths and controlled according to the obtained wavelength-switching scenarios. Control commands for switching wavelengths were sent to the WSS with 1100 ms interval time. The average connection holding time in this experiment is about several seconds, which is much shorter than that in practical optical communication networks. However, the time of several seconds is much longer than the response time of EDFA and is enough long for evaluating EDFA offset.

5.2. Results and Discussion

Some of the obtained waveforms are shown in Fig. 11. The vertical axis of each figure is intensity normalized by the maximum measured intensity during the whole measurement time for

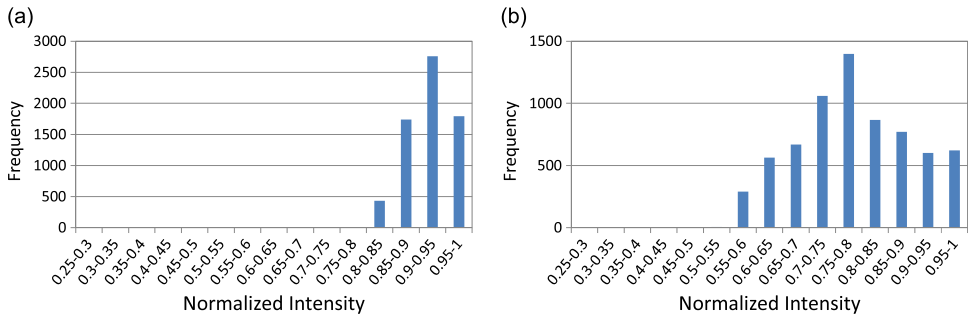

Fig. 12. Histograms of the normalized intensity of the light traffic pattern with the Random policy. (a) After one EDFA and (b) after five EDFAs.

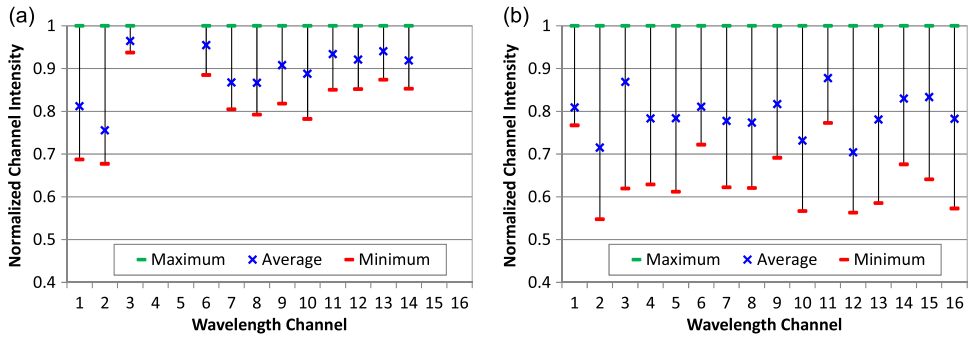

Fig. 13. Maximum, average, and minimum normalized channel intensity according to wavelength channels with the light traffic pattern after five EDFAs using (a) MinDiff policy and (b) Random policy.

each wavelength channel. Channel intensity changes are observed with dynamic switching of other wavelength channels because of the gain offsets. The waveforms (a) and (b) correspond to the Random policy after five EDFAs with Ch. 1 (1533.465 nm) and Ch. 8 (1544.526 nm), respectively. The fluctuations of the normalized intensity in (a) and (b) range from 0.52 to 1 and from 0.64 to 1, respectively. The waveforms (c) to (f) correspond to the MinDiff policy; (c) and (d) are after five EDFAs, while (e) and (f) are after one EDFA; (c) and (e) are wavelength Ch. 1 while (d) and (f) are wavelength Ch. 8. The fluctuations of the normalized intensity in (c), (d), (e), and (f) range from 0.69 to 1, from 0.81 to 1, from 0.89 to 1, and from 0.92 to 1, respectively. The waveforms after five EDFAs [(c) and (d)] experience larger intensity changes than those after one EDFA [(e) and (f)].

To evaluate the results in a statistical way, we counted the appearance frequency of the normalized intensity in each waveform with measurement intervals of 100 ms. Fig. 12 shows histograms of the normalized intensity for the case of the light traffic pattern with the Random policy. The spreads of the histograms represent the deviations of normalized channel intensity. Fig. 12 clearly shows that the channel intensity deviations after five EDFAs are larger than those after one EDFA, that is, the influence of the gain offsets accumulates.

The waveform of (c) in Fig. 11 suffers from slightly larger intensity deviations than that of (d). In addition, the calculated waveform is more in accordance with the measured waveform of Ch. 8 [(f) in Fig. 11] than of Ch.1 [(e) in Fig. 11]. Fig. 13 shows the normalized channel intensity distribution vs. wavelength channels observed with the light traffic pattern after five EDFAs. Regarding the MinDiff policy shown in Fig. 13(a), wavelength channels 1 and 2 experience larger intensity deviations than other channels. This occurs because the short wavelength channels have small differences between the gain for single-channel input $[g_S(\lambda)]$ and the gain for WDM input $[g(\lambda)]$; however, the gain offset the channel actually experiences can be large as implied

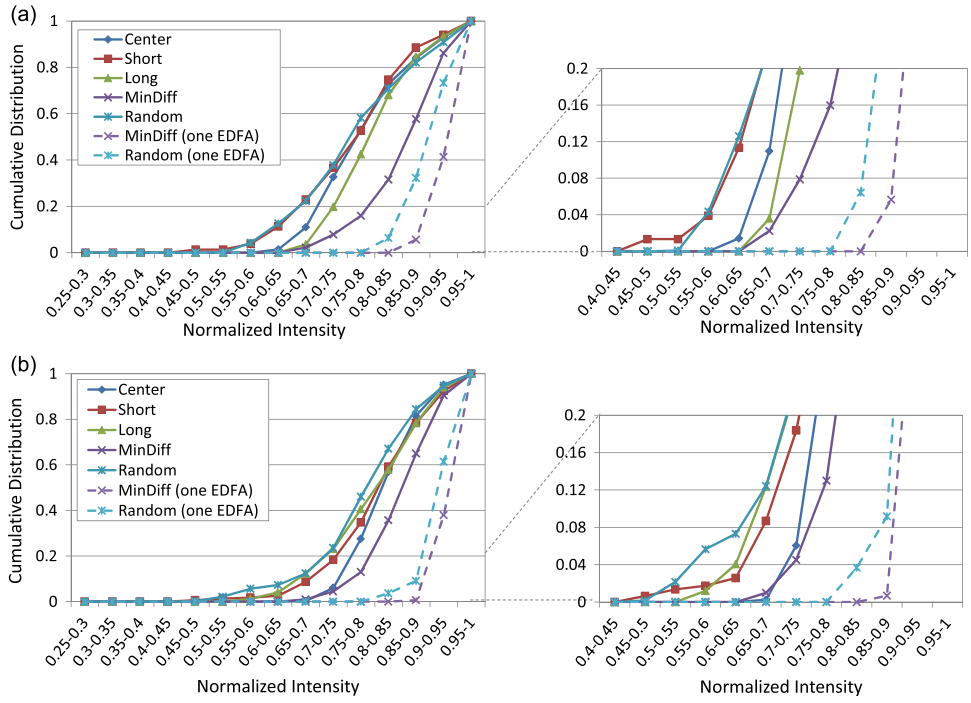

Fig. 14. Cumulative distributions of measured intensity deviations for (a) light traffic pattern and (b) heavy traffic pattern. The right-hand side graphs enlarge the vertical axes.

in Fig. 5. This discrepancy is caused by the fact that the gain model does not take into account the gain spectrum change because of the GSHB effect.

Fig. 14 shows the cumulative distributions of the observed intensity deviations. The five solid lines in each graph show the five wavelength assignment policies after five EDFAs, respectively. The two dashed lines in each graph show the Random policy and the MinDiff policy after one EDFA. The MinDiff policy offers the smallest deviations among the five policies. In addition, the MinDiff policy provides almost the same performance between the light traffic pattern (a) and the heavy traffic pattern (b), while the other policies have larger deviations in the light traffic pattern than in the heavy traffic pattern. Large gain changes tend to occur with large changes of EDFA input. The amount of the EDFA input change can be determined with the proportion of the number of newly established/deleted channels to that of the existing channels. Accordingly, the heavy traffic pattern experience relatively smaller changes of EDFA input than the light traffic pattern. So, the light traffic pattern generally suffers from larger gain changes, as shown in Fig. 14. However, since we have higher flexibility of wavelength assignment with the light traffic pattern than with the heavy traffic pattern, the MinDiff policy can eliminate the gain change on the light traffic pattern by considering the EDFA gain characteristics compared to the other policies.

The deviations after five EDFAs are 10–15% larger than those after one EDFA. The difference between the Random and the MinDiff policy is also larger after five EDFAs than after one EDFA. The MinDiff policy can reduce the gain deviations by 5 to 15%, namely, 0.3–0.7 dB, after cascading five EDFAs compared with the other policies. The reduction effect will become more significant as the number of cascaded EDFAs increases. It is not easy to determine the allowable range for the gain deviation; since it depends on the design of entire network systems. However, to operate agile and dynamic optical switching networks, a large gain change which occurs even less frequently should be avoided and the average gain deviation would need to be suppressed as much as possible.

Here we would like to note that the statistical graphs of Figs. 12–14 consider only the time when the wavelength channel is on. In other words, two types of period are excluded: 1) when

the wavelength channel is off and 2) during the transition of the optical switch when the wavelength channels between on and off. In the experiments, instantaneous transients were not observed since the switch speed of the WSS is much slower than the EDF response, and the EDFA we used here can effectively suppress the transients as evaluated in [16].

6. Conclusion

The gain offset of a WDM AGC EDFA with fast electrical feedforward control has been experimentally investigated under a condition of dynamic optical switching. Practical wavelength switching scenarios were generated by resolving dynamic RWA problems with two traffic patterns (a light and a heavy traffic pattern), and five wavelength assignment policies are examined: 1. Long, 2. Short, 3. Center, 4. Random, and 5. MinDiff. Dynamic changes of optical channel intensities were observed with dynamic wavelength switching because of the EDFA offset. Larger intensity deviations were observed after five EDFAs than after one EDFA; the effects of the EDFA offset accumulated. Larger intensity deviations were observed in the cases of the light traffic pattern than the heavy traffic pattern. The MinDiff policy, which considers a simple gain model, could provide the smallest channel intensity deviations among the five assignment policies. Since the gain model did not take into account the gain spectrum change caused by the GSHB, larger intensity deviations were observed for shorter wavelengths than for long wavelengths with the MinDiff policy. Even so, the MinDiff policy could successfully reduce the gain offsets by 5–15%, namely 0.3–0.7 dB, compared with the other policies, after five cascaded EDFAs. Because of its simple gain model, the MinDiff policy did not increase the computation complexity or computing time relative to the other policies. Future work may evaluate effects of dynamic optical channel intensity changes on system performances such as bit error rate or optical signal to noise ratio and clarify allowable ranges of the intensity changes to achieve a certain system performance.

Appendix

The detailed formulation of the establishment operation in the dynamic RWA used in Section 4 is described below. We formulated the problem by modifying the link ILP formulation shown in [21] to apply dynamic demands.

1) Notations and network parameters:
   - V Set of all nodes.
   - E Set of all fibers.
   - L Set of all wavelengths in a fiber.
   - D_{est} Set of all demands for establishment paths at an iteration.
   - s_k Source node of a demand $k \in D_{\text{est}}$.
   - d_k Destination node of a demand $k \in D_{\text{est}}$.
   - $A^-_{v_i}$ Set of fibers input to the node $v_i \in V$.
   - $A^+_{v_i}$ Set of fibers output from the node $v_i \in V$.
   - W_λ Weight for the wavelength λ, which is determined depending on the wavelength assignment policies that are described below.
   - O^λ_e Indicator for the wavelength resource utilization: 1 if the wavelength $\lambda \in L$ in the fiber $e \in E$ has been utilized by other demands in previous iterations; 0 otherwise.
2) Decision variables:
   - $x^\lambda_{k,e}$ 1 if the wavelength $\lambda \in L$ in the fiber $e \in E$ is assigned to accommodate the demand $k \in D_{\text{est}}$; 0 otherwise.
3) Objective

$$\text{minimizing} \sum_{\lambda \in L} \sum_{k \in D_{\text{est}}} \sum_{e \in E} x^\lambda_{k,e} + \sum_{e \in E} w_e. \tag{3}$$

4) Constraints:

$$\sum_{e\in A^{+}_{v_i}} x^{\lambda}_{k,e} = \sum_{e\in A^{-}_{v_i}} x^{\lambda}_{k,e} \quad \forall k \in D_{\text{est}},\ \forall v_i \in V/\{s_k, d_k\},\ \forall \lambda \in L \tag{4}$$

$$\sum_{\lambda\in L}\sum_{e\in A^{+}_{s_k}} x^{\lambda}_{k,e} = 1 \quad \forall k \in D_{\text{est}} \tag{5}$$

$$\sum_{\lambda\in L}\sum_{e\in A^{-}_{s_k}} x^{\lambda}_{k,e} = 0 \quad \forall k \in D_{\text{est}} \tag{6}$$

$$\sum_{\lambda\in L}\sum_{e\in A^{-}_{d_k}} x^{\lambda}_{k,e} = 1 \quad \forall k \in D_{\text{est}} \tag{7}$$

$$\sum_{\lambda\in L}\sum_{e\in A^{+}_{d_k}} x^{\lambda}_{k,e} = 0 \quad \forall k \in D_{\text{est}} \tag{8}$$

$$\sum_{k\in D_{\text{est}}} x^{\lambda}_{k,e} \le 1 - O^{\lambda}_{e} \quad \forall e \in E,\ \forall \lambda \in L \tag{9}$$

$$w_e \le W_\lambda x^{\lambda}_{k,e} \quad \forall e \in E,\ \forall \lambda \in L,\ \forall k \in D_{\text{est}}. \tag{10}$$

Constraints (4)–(8) correspond to the flow conservation constraints. Equation (4) also corresponds to the wavelength continuity constraints. Constraint (9) represents the wavelength clash constraints. Constraint (10) reflects the wavelength assignment policies; w_e represents a weight value of a fiber e, which is the maximum weight of the wavelength used in the fiber e.

The value of W_λ is determined according to the wavelength assignment policies. The range of W_λ is limited to [0,0.1) to avoid the use of extra wavelength resources as a result of applying the wavelength assignment policies. W_λ is given as follows:

1. Long: $W_\lambda > W_{\lambda+1} \quad \forall \lambda, \lambda+1 \in L$ (11)
2. Short: $W_\lambda < W_{\lambda+1} \quad \forall \lambda, \lambda+1 \in L$ (12)
3. Center: $\begin{cases} W_\lambda > W_{\lambda+1} & \forall \lambda, \lambda+1 \in L,\ \lambda \le \lambda_c \\ W_\lambda < W_{\lambda+1} & \forall \lambda, \lambda+1 \in L,\ \lambda \ge \lambda_c \end{cases}$ (13)
4. Random: W_λ is randomly determined at each iteration.
5. MinDiff: $W_\lambda = \alpha |g_s(\lambda) - g(\lambda)|$. (14)

λ_c in (13) represents the center wavelength. $g_s(\lambda)$ and $g(\lambda)$ in (14) are the measured values. α is an constant coefficient to ensure that $W_\lambda < 0.1$.

Acknowledgment

The authors thank Y. Oikawa, N. Sato, and N. Shiga of Trimatiz Ltd. for their informative discussions.

References

[1] K. Sato and H. Hasegawa, "Optical networking technologies that will create future bandwidth-abundant networks [invited]," *IEEE/OSA J. Opt. Commun. Netw.*, vol. 1, no. 2, pp. A81–A93, Jul. 2009.
[2] B. Collings, "New devices enabling software-defined optical networks," *IEEE Commun. Mag.*, vol. 51, no. 3, pp. 66–71, Mar. 2013.
[3] J. Kurumida *et al.,* "First demonstration of ultra-low-energy hierarchical multi-granular optical path network dynamically controlled through NSI-CS for video related applications," presented at the Eur. Conf. Opt. Commun., Cannes, France, 2014, Paper PD1.3.
[4] S. Y. Park, H. K. Kim, G. Y. Lyu, S. M. Kang, and S.-Y. Shin, "Dynamic gain and output power control in a gain-flattened erbium-doped fiber amplifier," *IEEE Photon. Technol. Lett.*, vol. 10, no. 6, pp. 787–789, Jun. 1998.
[5] G. Luo *et al.,* "Performance degradation of all-optical gain clamped EDFA's due to relaxation-oscillations and spectral hole burning in amplified WDM networks," *IEEE Photon. Technol. Lett.*, vol. 9, no. 10, pp. 1346–1348, Oct. 1997.

[6] J. Zyskind and A. Srivastava, *Optically Amplified WDM Networks: Principles and Practices*. San Diego, CA, USA: Academic, 2011.
[7] K. Okamura *et al.,* "Optical burst amplification using EDFA with fast feedback control," presented at the Opt. Fiber Commun. Conf., Anaheim, CA, USA, 2005, Paper OTuN2.
[8] A. Lieu, C. Tian, and T. Naito, "Transmission and interaction of WDM burst signals in cascaded EDFAs," presented at the Opt. Fiber Commun. Conf., Anaheim, CA, USA, 2006, Paper OTuD5.
[9] Y. Awaji, H. Furukawa, N. Wada, P. Chan, and R. Man, "Mitigation of transient response of erbium-doped fiber amplifier for burst traffic of high speed optical packets," presented at the Lasers Electro-Optics Conf., Baltimore, MD, USA, 2007, Paper JTuA133.
[10] B. J. Puttnam, Y. Awaji, and N. Wada, "Investigating the limits of optical packet transmission through cascaded transient-suppressed EDFAs without regeneration or active gain control," presented at the Opt. Fiber Commun. Conf., San Diego, CA, USA, 2010, Paper OThI6.
[11] N. Sato, K. Ota, N. Mishima, Y. Oikawa, and N. Shiga, "Less than 0.19-dB transient gain excursion AGC-EDFA with digital control for 20-channel add/drop equivalent operation," presented at the Opt. Fiber Commun. Conf., Los Angeles, CA, USA, 2011, Paper OMH3.
[12] A. Kaszubowska-Anandarajah *et al.,* "EDFA transient suppression in optical burst switching systems," presented at the Proc. 14th Int. Conf. Transparent Opt. Networks, Coventry, U.K., 2012, Paper Mo.B2.4.
[13] L. Rapp, "Transient performance of erbium-doped fiber amplifiers using anew feedforward control taking into account wavelength dependence," *J. Opt. Commun.*, vol. 28, no. 2, pp. 82–90, Jun. 2007.
[14] B. Dumas and R. Olivares, "Transient link control technique applied to optical hybrid amplifier (EDFA+DFRA) cascades," *J. Opt. Commun. Netw.*, vol. 4, no. 11, pp. 858–864, Nov. 2012.
[15] K. Ishii *et al.,* "Suppression of transients in an EDFA chain using feed-forward pump control and a high-speed VOA," presented at the Opt. Fiber Commun. Conf., Los Angeles, CA, USA, 2012, Paper OW4D.4.
[16] K. Ishii *et al.,* "Experimental investigation of transients in six cascaded AGC EDFAs and their suppression using a high-speed VOA," *IEICE Commun. Exp.*, vol. 1, no. 4, pp. 137–142, 2012.
[17] M. Bolshtyansky and G. Cowle, "Spectral hole burning in EDFA under various channel load conditions," presented at the Opt. Fiber Commun. Conf., San Diego, CA, USA, 2009, Paper OTuH5.
[18] M. Nishihara, Y. Sugaya, and E. Ishikawa, "Impact of spectral hole burning in multi-channel amplification of EDFA," presented at the Opt. Fiber Commun. Conf., Los Angeles, CA, USA, 2004, Paper FB1.
[19] K. Ishii, J. Kurumida, and S. Namiki, "Wavelength assignment dependency of AGC EDFA gain offset under dynamic optical circuit switching," presented at the Opt. Fiber Commun. Conf., San Francisco, CA, USA, 2014, Paper W3E.4.
[20] Y. Oikawa, N. Sato, K. Ota, S. Petit, and N. Shiga, "0.2-dB gain excursion AGC-EDFA with a high speed VOA for 100-channel add/drop equivalent operation," presented at the Opt. Fiber Commun. Conf., Los Angeles, CA, USA, 2012, Paper OW4D.3.
[21] B. Jaumard, C. Meyer, and B. Thiongane, "Comparison of ILP formulations for the RWA problem," *Opt. Switching Netw.*, vol. 4, no. 3/4, pp. 157–172, Nov. 2007.
[22] E. Desurvire, J. L. Zyskind, and J. R. Simpson, "Spectral gain hole burning at 1.53 μm in erbium-doped fiber amplifiers," *IEEE Photon. Technol. Lett.*, vol. 2, no. 4, pp. 246–248, Apr. 1990.
[23] E. Desurvire, C. R. Giles, and J. R. Simpson, "Gain saturation effects in high-speed, multichannel erbium-doped fiber amplifiers at $\lambda = 1.53$ μm," *J. Lightw. Technol.*, vol. 7, no. 12, pp. 2095–2104, Dec. 1989.
[24] R. Peretti, A. M. Jurdyc, B. Jacquier, E. Burov, and L. Gasca, "Resonant fluorescence line narrowing and gain spectral hole burning in erbium-doped fiber amplifier," *J. Luminescence*, vol. 128, no. 5/6, pp. 1010–1012, May/Jun. 2008.
[25] R. Peretti, B. Jacquier, D. Boivin, E. Burov, and A. M. Jurdyc, "Inhomogeneous gain saturation in EDF: Experiment and modeling," *J. Lightw. Technol.*, vol. 29, no. 10, pp. 1445–1452, May 2011.
[26] K. Ishii, K. Tanizawa, J. Kurumida, and S. Namiki, "Experimental study of wavelength-dependent dynamic gain offsets of AGC WDM EDFA," presented at the OptoElectron. Commun. Conf. Photonics Switching, Kyoto, Japan, 2013, Paper WS3-1.
[27] *Trimatiz Data Sheets*. [Online] Available: http://www.trimatiz.com/up/pdf/products/BMAC-014JP.pdf